

# BULK NIOBUM POLISHING AND ELECTROPOLISHING STEPS FOR THINFILM COATED COPPER SRF CAVITIES\*

Mahadevan Krishnan<sup>#</sup>, Irfan Irfan, Steve Chapman and Katherine Velas,  
Alameda Applied Sciences Corporation, San Leandro, CA, USA

Joshua Spradlin and Hui Tian, Jefferson National Accelerator Facility, Newport News, VA

## Abstract

Alameda Applied Sciences Corporation (AASC) grows Nb thin films via Coaxial Energetic Deposition (CED) from a cathodic arc plasma. The plasma consists of 60-120eV Nb ions (Nb<sup>+</sup> and Nb<sup>++</sup>) [1] that penetrate a few monolayers into the substrate [2] and enable sufficient surface mobility to ensure that the lowest energy state (crystalline structure with minimal defects) is accessible to the film [3]. One limitation of CED thinfilms is the presence of Nb macroparticles (~0.1-10 microns) that could be deleterious to high field performance of the SRF cavity. One way to remove such macroparticles [4] is to grow a thick film (~3-5 microns), followed by mechanical polishing (MP) using the finest media as might be applied in Centrifugal Barrel Polishing (CBP) to achieve a 0.4 micron surface figure, and an electropolishing (EP) step to remove ~1 micron of Nb that also removes all traces of embedded media in the film. The residual 2-4 micron Nb film should more nearly resemble the surface of a bulk Nb cavity that has been subjected to the same steps. This paper describes experiments conducted on Cu coupons as a prelude to an SRF Cu cavity coating.

## INTRODUCTION

In the early 1980s, researchers at CERN [5] explored the concept of sputtered films of Nb on copper cavities as a potential replacement for bulk Nb SRF cavities.  $Q_0$  values in excess of  $2 \times 10^9$  at 5 MV/m were reproducibly achieved on single cell 500 MHz cavities and a  $Q_0$  value of  $6.2 \times 10^9$  was reached at 5 MV/m on a 4 cell 352 MHz cavity. These excellent results were tempered by the sporadic appearance of blisters in the Nb film and a rapid decrease of  $Q_0$  with increasing field (called Q-slope). Papers published in the 1990s [6,7] suggested that impurities in the film were responsible for the drop in Q with higher field. In the early 2000s, Langner [8] Russo [9] and others proposed the use of cathodic arcs to grow the Nb thin films. This pioneering work was motivated by the fact that cathodic arcs naturally generate ions that are energetic (60-120eV) as compared to the ~1eV ions from magnetron guns. The more energetic ions would presumably lead to denser (less porous) films with better adhesion. Furthermore, the source of ions from an ultrahigh vacuum might also be conducive to purer

films with better SRF properties. Residual Resistivity Ratio (RRR) of up to 100 was measured in Nb films grown at substrate temperatures of ~100 °C. RF cavity cells were coated using various configurations of cathodic arcs. These early attempts did not demonstrate high  $Q_0$  either due to poor surface preparation or impurities in the film.

There are three types of plasma sources that use energetic ions to grow thin films: cathodic arcs, Electron Cyclotron Resonance (ECR) plasmas and High Power Impulse Magnetron Sputtering (HiPIMS). All three sources produce dense, well adhered films and have therefore been actively pursued for better SRF cavity coating applications. This paper presents results using cathodic arcs. Our earlier work on coupons of a-sapphire and MgO [1] motivated coating of Nb films on Cu coupons and has recently progressed to coating 1.3 GHz RF cavities.

This paper focuses on the problem of macroparticles in the thin films that are grown using cathodic arc deposition. Macroparticles are neutral droplets ranging in size from ~0.1-10  $\mu\text{m}$  in all cathodic arcs, ejected from molten craters [10] as cathode spots extinguish. With regard to the magnetic field, these macroparticles could allow vortex penetration if the thermal conductivity from the macroparticle to the underlying Nb thinfilm is poor. With regard to the electric field, the protrusion of the macroparticles from the thinfilm surface could cause field enhancement and cavity breakdown at lower fields than required. Figure 1 shows a cross-section SEM of a typical Nb macroparticle on a 2.43  $\mu\text{m}$  thick Nb film grown using CED.

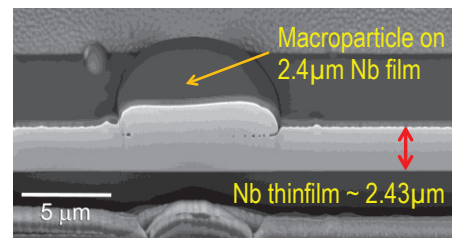


Figure 1: Cross-section SEM of Nb thinfilm showing an embedded macroparticle.

XRD analysis of the film showed that the film was a Nb crystal with {100} orientation. The macroparticle also showed the same crystalline structure and is obviously well adhered to the film. The macroparticle is ejected from the crater of the cathode spot and is at the melt temperature when it lands on the film (the flight time from cathode to substrate is short enough

Work supported by DOE SBIR  
Grant #DE-SC0011371  
#krishnan@aaasc.net

that no significant radiative cooling occurs in flight). Thus the macroparticle cools from melt and adopts the crystallinity of the underlying material, which in this case is {100} Nb. It is reasonable to suppose that the thermal conduction from macroparticle to underlying Nb film is as good as that of the film itself, so there should be no magnetic field penetration issue due to macroparticles. However, the radius of the macroparticle at the edges creates an electric field enhancement that could be a limitation.

A chance conversation with Dr. Hasan Padamsee of Fermilab led to his suggesting that one way to mitigate the electric field enhancement due to macroparticles would be to begin with a thick Nb film, say 3-5  $\mu\text{m}$ , then perform a centrifugal barrel polishing (CBP) step using the finest media ( $\sim 50$  nm), to dislodge the weakly adhered macroparticles and grind the others down to the underlying surface. This polishing step would be followed by an electropolishing (EP) step, in which approximately  $1\mu\text{m}$  of Nb would be etched away, to remove all traces of any embedded CBP polishing media in the film. These two post-coating steps would produce a thinfilm surface with about the same surface figure as that of a bulk Nb cavity that is subjected to the same steps, though for bulk cavities, the CBP is more elaborate, starting with coarser media and culminating in the final ( $0.4\mu\text{m}$  surface figure) step. As a prelude to testing this idea on an RF cavity, we decided to test the concept using 37 mm Cu disks. Since CBP cannot be performed on a 37 mm disks, a parallel process using similar final slurry was performed on a Buehler Ecomet 300 with 50 nm Colloidal  $\text{Al}_2\text{O}_3$ .

## COATING PROCEDURE

Figure 2 shows a photograph of the Coaxial Energetic Condensation (CED) apparatus. Base pressures of  $\sim 10^{-8}$  Torr are possible within this chamber and are measured and monitored using a SRS200 residual gas analyser. In addition to substrate temperature control, the substrate can also be biased. The key process variables are substrate temperature, degree of annealing, substrate bias, deposition rate, and base pressure. Figure 3 shows the interior details.

Two heater plates were mounted at a distance of 40 mm from the axis of the 12.7 mm Nb cathode. The 37 mm Cu disks were mounted on the heater plates to heat one disk (designated as 001) to  $150^\circ\text{C}$ , while the other two (002 and 003) were heated to  $300^\circ\text{C}$ . Disks 001 and 003 were also biased to  $-40$  V, to accelerate the incoming Nb ions (60-120 eV incident energy) to 100-160 eV ( $\text{Nb}^+$  ions) or 140-200 eV ( $\text{Nb}^{2+}$  ions). A total of 20,000 shots was fired at an arc current of 150 A to grow a  $\approx 5\mu\text{m}$  thick Nb film on the three Cu disks.

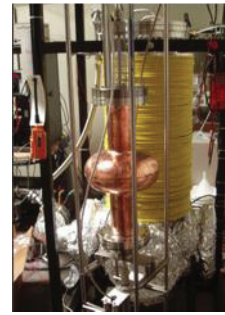


Figure 2: Photograph of the CED apparatus, with a 2.2 GHz RF cavity shown for scale.

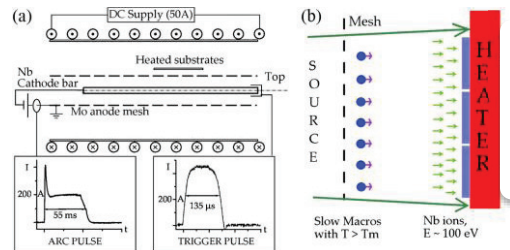


Figure 3: Schematic drawing of CED operation: (a) Coaxial geometry and typical current pulses to the trigger and the arc; (b) shows plasma transmitted by the anode onto the substrate.

The Cu disks were prepared in batches of 10 by MP using several steps:

- [1] SiC 320 grit 10 lbs down force 90 rpm base 60 rpm base until plane
- [2] SiC 400 grit 10 lbs down force 90 rpm base 60 rpm base for  $\sim 10$  min  $\sim 8$  papers 1.5 min / paper
- [3] SiC 600 grit 10 lbs down force 90 rpm base 60 rpm base for  $\sim 10$  min  $\sim 8$  papers
- [4]  $9\mu\text{m}$   $\text{Al}_2\text{O}_3$  10 lbs down force 90 rpm base 60 rpm head for 5 min  $\sim 3$  papers
- [5]  $3\mu\text{m}$   $\text{Al}_2\text{O}_3$  10 lbs down force 90 rpm base 60 rpm head for 5 min  $\sim 3$  papers
- [6] Synthetic nap cloth  $3\mu\text{m}$  diamond slurry 120 rpm base 120 rpm head 25 lbs down force 20 min 2 pads

The Nb CED thin films on Cu were polished using two steps:

- [1] 5 min with 50 lbf 90 rpm base 60 rpm head for 3 min using a Buehler TextMet Pad and Allied High Tech 50 nm Colloidal  $\text{Al}_2\text{O}_3$
- [2] 10 min with 50 lbf 90 rpm base 60 rpm head for 7 min using a Buehler MasterMet and Allied High Tech 50 nm Colloidal  $\text{Al}_2\text{O}_3$

The EP step used 10:1  $\text{H}_2\text{SO}_4$  (98%): HF (49%), at 10V, 5 min,  $\sim 0.05\text{A}$  per sample. By precise control of the bath temperature and the electrolyte concentration, it was possible to remove only  $\approx 0.9\mu\text{m}$  ( $0.87\mu\text{m}$  was calculated) from the thinfilm. The combination of fine MP and precisely controlled EP were both key factors for successful implementation of Padamsee's idea.

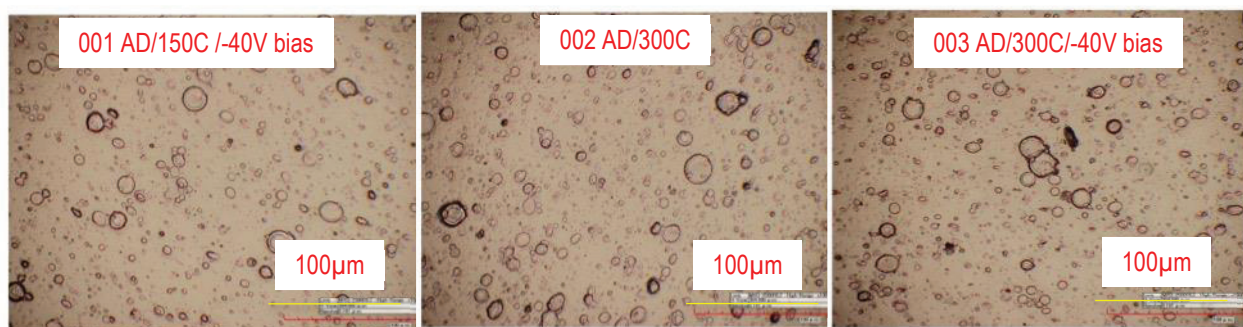


Figure 4: HiROX digital microscope images of Cu 001 (150C with -40V bias), 002 (300C) and 003 (300C with -40V bias) coupons as deposited (AD) with  $\approx 5 \mu\text{m}$  Nb.

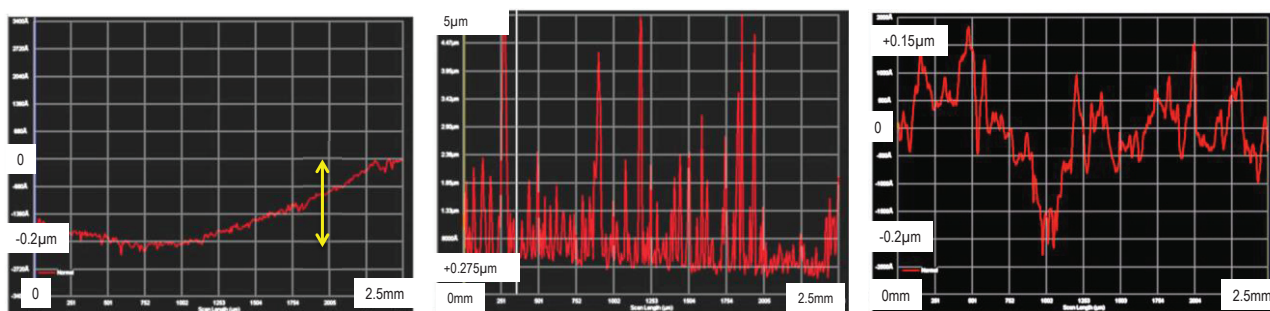


Figure 5: Profilometer traces: Left: of the Cu coupon after MP; Middle: of the coated Nb film as deposited (AD); Right: of the coated Nb film after mechanical polishing (MP) and electropolishing (EP).

## RESULTS

### Optical Microscope Images of Nb Films

A HiROX digital imaging microscope [11] was used to image the Nb films from the three coupons 001, 002 and 003. Figure 4 shows the HIROX images. The images in Fig. 4 show that macroparticles of up to  $20 \mu\text{m}$  in size are present on the coupons regardless of coating temperature or bias conditions. This is as expected since the macroparticles are molten, charge neutral droplets of Nb. By comparison with the cross-section SEM image of Fig. 1, it is observed that the macroparticles are not spherical when deposited, but flattened to look like platelets. The height of a macroparticle is much less than its diameter.

Figure 5 shows three profilometer scans: (left) across the bare Cu substrate (after MP); (middle) across the Nb coated Cu 001 coupon; (right) across the coated Cu 001 after the MP and EP steps described above. The global variation of the surface of the bare Cu coupon across a  $2.5 \text{ mm}$  field of view is  $\sim 0.2 \mu\text{m}$ , to which we must compare the profile after the coating, MP and EP steps. The middle profilometer trace shows that the roughness of the as coated film is  $\approx 4.75 \mu\text{m}$  (the baseline of the scan is not at zero but at  $0.275 \mu\text{m}$ ). As stated earlier, this scan shows that the macroparticles are flattened with heights above the base film of  $\approx 5 \mu\text{m}$  and diameter up to  $20 \mu\text{m}$ .

The right profilometer trace shows that the MP and EP steps remove the macroparticles and leave a Nb

surface with a surface roughness of  $\approx 0.35 \mu\text{m}$ . It is of interest to compare this result with the surface figure that is typical of bulk Nb cavities. Figure 6 [12] shows HiROX digital microscopy images of a sample of polycrystalline Nb as used in bulk Nb SRF cavities, after BCP (upper) and EP (lower) treatments.

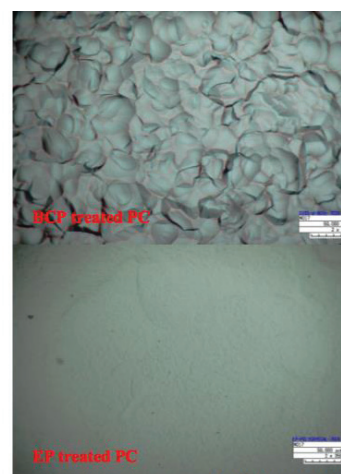


Figure 6: HiROX images of a bulk Nb cavity surface that was buffered chemically etched (BCP) and then electropolished (from ref. 12).

The BCP treated poly-Nb was heavily etched and shows an RMS roughness of  $\sim 1.6 \pm 0.42 \mu\text{m}$  across a  $50 \mu\text{m} \times 50 \mu\text{m}$  field of view. The EP treated poly-Nb shows an RMS roughness of  $\sim 0.34 \pm 0.11 \mu\text{m}$  across

the same  $50\ \mu\text{m} \times 50\ \mu\text{m}$  region. If we use this RMS roughness of  $\sim 0.34\ \mu\text{m}$  as a standard, *our Nb film after MP and EP meets that criterion, as our peak-peak roughness is  $\approx 0.35\ \mu\text{m}$ .*

### SEM/EBSD Images

Figure 7 shows Scanning Electron Microscope (SEM), Electron Backscatter Diffraction (EBSD) and Inverse Pole Figure (IPF) images of sample 001 after the initial MP (left image) and EP (right image) steps.

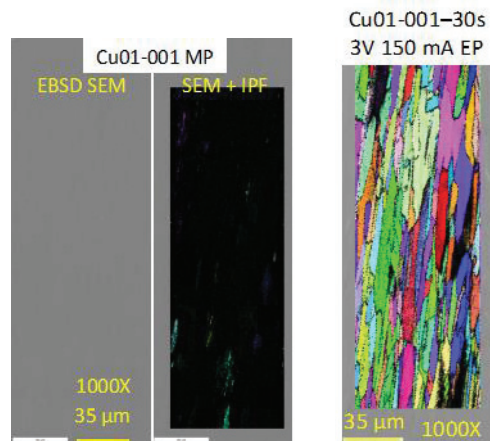


Figure 7: SEM/EBSD images of Cu 001 coupon after mechanical polishing (MP, left) and after electropolishing (EP, right).

Figure 8 shows similar images taken from coated (AD) Cu 001 (left) and after the MP step (right). The left SEM image shows macroparticles all over the surface.

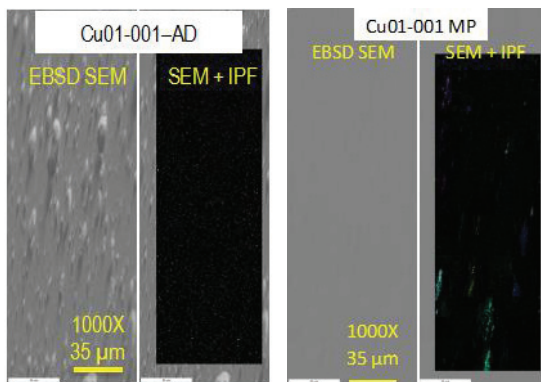


Figure 8: SEM/EBSD images of coated Cu 001 coupon (left) and after MP (right).

The IPF image in Fig. 7 after EP reveals polycrystalline Cu grains ( $\sim 10\ \mu\text{m}$  in size) of various orientations. The  $35\ \mu\text{m}$  resolution in the SEM image serves as a comparison reference for what follows with the Nb coated samples. By contrast, the IPF image of Cu 001 with the Nb film (Fig. 8) shows no crystalline Nb (the black color indicates too low a confidence index for the EBSD signal). There are occasional tiny spots that might suggest nano-crystallites, possibly due to condensation of macroparticles. One possible reason

for this is that we did not pre-heat the coupons to  $>400\text{C}$  for many hours as we have in the past, to dissolve the oxide film at the copper surface. As a consequence, these Nb films were grown on an amorphous oxide surface and so heteroepitaxial growth did not occur. It is not yet known how important a crystalline structure is for good RF performance. What matters more is a defect free (or very low defect) Nb film that offers low residual resistance at  $<4\text{K}$ .

Figure 9 shows similar images for Cu 002. Figure 10 shows the images for Cu 003.

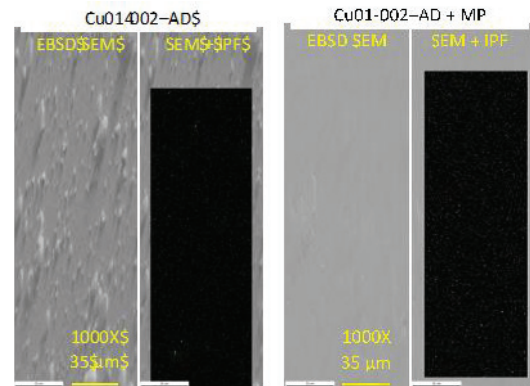


Figure 9: SEM/EBSD and IPF images of coated Cu 002 (AD, left) and after MP (right).

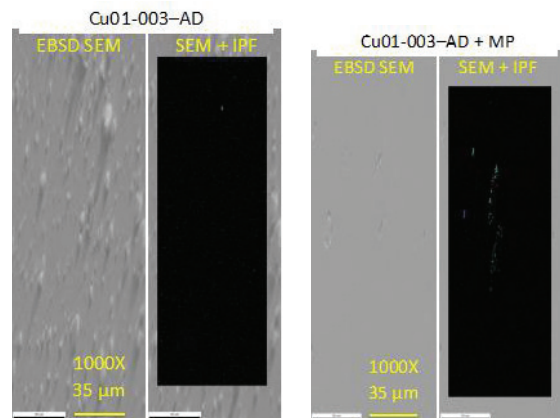


Figure 10: SEM/EBSD and IPF images of coated Cu 003 coupon (AD, left) and after MP (right).

In all three cases the SEM images on the scale of  $35\ \mu\text{m}$  show that the MP step removes macroparticles and leaves behind a smooth Nb surface. This smoothness was quantified by the profilometer scans in Fig. 5.

Just as the HiROX images showed no significant difference between the three coating conditions as far as macroparticles are concerned, the SEM images also indicate that the surface figure of the Nb films after MP is about the same for all three coupons. This was verified by examination of the profilometer scans for all three coupons (not shown here).

## CONCLUSION

This paper has presented a new technique to remove macroparticles from Nb thinfilms. The technique was demonstrated on 37 mm Cu coupons, but it is straightforward to implement it on SRF elliptical cavities. For a cavity, the MP step would be replaced by a CBP step, still using the finest media. The EP step would remain substantially the same.

Past efforts in cavity coating have indicated that cavity surface preparation is extremely important for the success of a niobium deposition. A companion paper [13] shows that the same procedures that are used to prepare a bulk Nb SRF cavity have been applied to a copper cavity supplied to AASC by Fermilab. The cavity will soon be coated at AASC and tested at Fermilab. We will use a variable transmission anode [13] to create a film of uniform thickness in the equator and beam tube regions of the 1.3 GHz cavity. Additional cavities will be coated in partnership with Fermilab and JLab. Once these cavities are RF tested, we will know the magnitude of the problem (if any) caused by the ubiquitous macroparticles in cathodic arc deposition. Should we encounter  $Q_0$  vs. E limitations attributable to macroparticles, we will use the techniques described in this paper to remove macros and hopefully reach the elusive goal of  $Q_0 > 10^{10}$  out to  $E > 20$  MV/m.

## ACKNOWLEDGMENT

We are grateful to Dr. Hasan Padamsee for suggesting this technique for macroparticle removal and to the US DOE SBIR program for financial support. Work at AASC was supported by DOE SBIR Grant #DE-SC001137. The JLab effort was supported by the U.S. Department of Energy, Office of Science, Office of Nuclear Physics under contract DE-AC05-06OR23177. The HiROX images are courtesy of the College of William and Mary Surface Characterization Laboratory.

## REFERENCES

- [1] A. Bendavid, P. J. Martin, R. P. Netterfield, G. J. Sloggett, T. J. Kinder, C., Andrikidis, Journal of Materials Science Letters 12 (1993) 322-323.
- [2] Y. Lifshitz, S. R. Kasi, J. W. Rabalais, and W. Eckstein, Phys. Rev. B 41, 10468 (1990).
- [3] Krishnan, Mahadevan; Valderrama, E; James, C; Zhao, X; Spradlin, J; Valente Feliciano, A.M; Phillips, L; Reece, C.E.; Seo, K; Sung, Z.H., Physical Review Special Topics-Accelerators and Beams, 15, 3, 32001, (2012).
- [4] Idea suggested by Dr. H. Padamsee of FNAL
- [5] C. Benvenuti, N. Circelli, M. Hauer, Appl. Phys. Lett. 45, 1984. 583.
- [6] C. Benvenuti, Part. Accel. 40 1992. 43.
- [7] C. Benvenuti, S. Calatroni, I.E. Campisi, P. Darriulat, M.A. Peck, R. Russo, A.-M. Valente, Physica C316, 1999, 153–188, (Elsevier).

- [8] J. Langner, TESLA Rep. 2000-15, D. Proch, DESY 2000.
- [9] R. Russo et al, Supercond. Sci. Technol. 18 (2005) L41-L44.
- [10] A. Anders, Cathodic Arcs, From Fractal Spots to Energetic Condensation, Springer Series on Atomic, Optical, and Plasma Physics, Vol. 50.
- [11] Digital Microscope System built by HiROX Corporation of Japan.
- [12] Hui-Tian presentation from: <http://uspas.fnal.gov/materials/08UMD/SRF/SurfaceStudies.pdf>
- [13] K. Velas, I. Irfan, M. Krishnan and S. Chapman, Energetic Condensation Growth of Nb on Cu SRF Cavities, these proceedings, SRF2015 Whistler, Canada, TUPB032.